

Article

Solution of an Electrodynamics Problem for a Homogeneous Equivalent Segment of a Coaxial Load, Considering Heat Losses in the Conductors

Polina V. Tatarenko and Alexander S. Tatarenko * 

Department of Electronic Systems, Saint Petersburg Mining University, 199106 St. Petersburg, Russia

* Correspondence: tatarenko_as@pers.spmi.ru

Abstract: Mathematical aspects of solving an electrodynamic problem in the field of designing coaxial devices in the microwave range are considered. The solution of the electrodynamic problem for a homogeneous equivalent segment of a coaxial load in the single-mode approximation, considering the heat losses in the central and outer conductors, was obtained. A mathematical model of the microwave load, linking the high-frequency and design-technological parameters of the device, was built. To refine the model, we consider second-order effects associated with considering inhomogeneities that occur in places where the cross-section of the coaxial structure changes. The design of the 50- Ω load and the results of its experimental investigation are presented for comparison with theoretical calculations.

Keywords: differential equations; electrodynamic; mathematical model; microwave devices; coaxial structure

MSC: 65M99; 78A25; 78A55



Citation: Tatarenko, P.V.; Tatarenko, A.S. Solution of an Electrodynamics Problem for a Homogeneous Equivalent Segment of a Coaxial Load, Considering Heat Losses in the Conductors. *Mathematics* **2022**, *10*, 4732. <https://doi.org/10.3390/math10244732>

Academic Editors: André Nicolet and Guillaume Demésy

Received: 12 October 2022

Accepted: 9 December 2022

Published: 13 December 2022

Publisher's Note: MDPI stays neutral with regard to jurisdictional claims in published maps and institutional affiliations.



Copyright: © 2022 by the authors. Licensee MDPI, Basel, Switzerland. This article is an open access article distributed under the terms and conditions of the Creative Commons Attribution (CC BY) license (<https://creativecommons.org/licenses/by/4.0/>).

1. Introduction

A mathematical model and a carefully implemented computational experiment can significantly reduce the cost of a task's solution in electronics. Microwave electronics is rapidly evolving to meet today's modern needs. Many new designs of antennas [1–3], antenna arrays [4,5], filters [6,7], phase shifters [8,9], resonators [10], delay lines [11], sensor arrays [12] and other devices have been presented in recent studies. One of the main areas of research is miniaturization entailing searching for new designs [13] or materials [14]. Modern research in the field of microwave devices has also increased the need to search for new modeling methods [15,16], which can be divided into methods of synthesis [17,18] and analysis [19]. The most accurate results can be obtained using analytical methods. However, it is often quite difficult or impossible to create an exact mathematical model of the desired microwave devices. The method proposed in this study can be applied to the development of a wide range of microwave devices. The method is thoroughly tested. One of the most dynamic directions in the development of modern electronics concerns microwave device design and research. The equivalent circuits method is popular in microwave device design applications. It has become pertinent due to the generalization and development of the impedance concept in linear low-frequency circuits theory. There are many methods for solving microwave device design problems. One of the methods involves consideration of the electrodynamic problems faced.

One of the problems in microwave technology is the design of broadband, especially ultra-wideband, systems with a frequency overlap of several octaves or more. Work in this area has been going on for a long time, but the problem remains relevant because of the continual modernization of existing equipment, the development of ever higher frequencies, and the design of new systems. Improvements in technology make it possible

to obtain more miniature microwave components; therefore, equipment developers must develop new methods of calculation and use automated design systems.

A coaxial transmission line, and devices based on it, represents one of the most common structures used in microwave devices. There are several engineering approaches to calculating the parameters of coaxial structures. N. Markuvitz [20] derived an approximate solution using the small aperture method, processing all higher modes with plane-parallel approximations. H. E. Green [21] and L. Young [22] considered the problem numerically for very low frequencies. The least-squares boundary residuals method was used by R. Jansen [23] for numerical solution of the problem. The problem can also be solved using a mode-matching method, in which the fields on either side of the discontinuity in the coaxial line are decomposed into an infinite series of modes matched across the boundary to maintain continuity. This approach was used by Winnery and his collaborators [24] when analyzing a sharp change in the diameter of the inner conductor of coaxial lines. Solving the field equation gives the equivalent conductivity without any restrictions.

However, some problems associated with the design of microwave devices have been solved using an electrodynamic approach based on solving Maxwell's equations; several methods exist. Numerical methods have become especially relevant in recent years. Use of the method of solving Maxwell's equations in the time domain as a tool for the analysis of microwave systems is becoming increasingly important. One of the main advantages of the time domain method is its ability to model electromagnetic fields of arbitrary geometry over a wide frequency band.

However, simpler methods are applicable to microwave devices that are simple in terms of design. The present article discusses the mathematical aspects of solving an electrodynamic problem when designing coaxial microwave devices in the microwave range. An ultra-wideband coaxial matched 50-ohm load is used as an example. The solution to the electrodynamic problem for a homogeneous equivalent segment of a coaxial load is obtained. The heat losses in the central and outer conductors are considered. A theoretical research method for compiling a mathematical model of the load is presented. This method relates the high-frequency and design-technological device parameters. A mathematical model of the coaxial load is constructed. The load design and the experimental research are presented for comparison with the results of theoretical calculations. The presented method is quite general, but the obtained results show that the analysis is accurate over a wide frequency range.

The coaxial microwave devices theory developed makes it possible to obtain necessary practical application data. The article presents the calculation and design stages of a 50-ohm coaxial load in the microwave range. The main microwave load parameters are:

- the input resistance of a microwave transmission line section and its dependence on the design and technological parameters and the signal frequency;
- the microwave transmission line section standing-wave ratio;
- the microwave signal thermal power loss;
- dimensions and weight.

The relationship between the high-frequency and the structural-technological parameters of the load was investigated. The wave attenuation coefficient, considering the material parameters of the conductors and the device design features, as well as the standing wave coefficient expression, was obtained. An analysis of the obtained expressions was carried out.

The results obtained can also be applied to the calculation of various strip devices often used in microwaves. A strip line can be considered because of the evolution of a coaxial line [25]. A coaxial line with a circular cross-section is deformed so that, first, the cross-section of its inner and outer conductors becomes square, and then rectangular. Following this, the narrow walls of the outer conductor are removed to infinity; the result is a strip-line transmission line. Such a line is symmetrical; however, if you remove one of the outer plates, an asymmetrical strip line is obtained. Strip lines can have both dielectric and air filling. However, despite the physical simplicity of strip-line transmission systems,

a rigorous analysis of their properties is difficult. The main type of wave must be found by directly solving Maxwell’s equations under boundary conditions corresponding to a given design. Analogs of most coaxial and waveguide microwave elements can be designed for strip-line systems. Since such systems have a large bandwidth, complex circuits can be easily constructed from them. The advantages of strip lines include their relatively small size, low weight and the possibility of cheap mass production using printing technology.

2. Theoretical Method of Research Coaxial Load at Microwave

2.1. Quasi-Stationary Conditions of the Problem

A variety of mathematical methods are used to solve practical problems in microwave technology. A productive approach to the formulation and solution of problems is the use of classical circuit theory methods. In general, the problem of studying coaxial microwave devices can be formulated as follows: it is required to find a solution of Maxwell’s equations in a region bounded by a conducting surface that satisfies boundary conditions on this surface that relate electric and magnetic fields to surface densities of electric currents and charges or to surface impedance.

There is a wide range of frequencies in which Maxwell’s equations can be simplified. The total electromagnetic field is replaced by a quasi-stationary field. Such a replacement enables the equations of the electromagnetic field for the case of a system of linear conductors to be obtained in the form of equations in total derivatives with constant coefficients, which, as is known from the general theory of differential equations, are reduced to a system of algebraic equations.

Replacing the electromagnetic field by a quasi-stationary field is possible when the so-called quasi-stationarity conditions are met. The first quasi-stationarity condition is determined by the relation:

$$T \gg \tau; (\tau = \frac{L}{v_\varphi}), \tag{1}$$

where T is the period of electromagnetic oscillations, τ is the delay time, L is the linear dimensions of the device, and v_φ is the phase speed of an electromagnetic wave in the transmission line under consideration.

The second condition for quasi-stationarity is the expression:

$$\vec{j} \gg \frac{\partial \vec{D}}{\partial t}, \tag{2}$$

where \vec{j} is the conduction current density vector and \vec{D} is the electric induction vector.

From the second condition, it is possible to obtain a connection between the minimum period of electromagnetic field change and the technological coaxial load parameters:

$$\vec{j} = \sigma \vec{E}; \vec{D} = \epsilon \vec{E}, \Rightarrow, \sigma \vec{E} \gg \epsilon \frac{\partial \vec{E}}{\partial t}, (\epsilon \frac{\partial \vec{E}}{\partial t} = \epsilon \omega \vec{E}), \text{ or } T_{\min} \gg \frac{\epsilon}{\sigma} \tag{3}$$

where \vec{E} is the electric field strength, ϵ is the absolute permittivity of the coaxial filling, σ is the electrical conductivity of the conductor’s material (or coating material), ω is the frequency, and T_{\min} is the minimum period of the electromagnetic field change.

When inequality (2) is satisfied, the displacement current can be neglected with respect to the conduction current.

The third condition for quasi-stationarity is the requirement that the quantities characterizing the properties of the medium- σ , ϵ and μ , have the same values as in constant fields.

For ordinary macroscopic systems containing metals as conductors, the quasi-stationarity conditions are satisfied up to frequencies lying in the infrared part of the spectrum. The main condition for quasi-stationarity for coaxial loads is represented in Expression (1).

2.2. Differential Equations Derivation in the Quasi-Static Approximation for a Homogeneous Coaxial Line Section

The equivalent microwave load circuit can be represented as a cascade connection of homogeneous sections of transmission lines with equivalent parameters determined by the design and technological parameters of the load. Therefore, the analysis begins with the differential equation’s derivation [26] for a homogeneous coaxial load section.

Let us designate the capacitance, inductance, active resistance, and active conductivity per unit length of a homogeneous load section (linear values), respectively, as C_0 , L_0 , R_0 , and G_0 .

The expression for the voltage between the central and outer conductors in a homogeneous section, and the expression for the current along a homogeneous section of the load, can be obtained from Maxwell’s equations. These equations are known as telegraph equations [27].

$$-\frac{\partial U(z, t)}{\partial z} = R_0 i(z, t) + L_0 \frac{\partial i(z, t)}{\partial t} \tag{4}$$

Expression (4) can be interpreted as follows: the voltage between the central and outer conductors along a homogeneous section change, since the resistance of this section determines the ohmic voltage drop, and its inductance, determines the inductive voltage drop.

$$\frac{\partial i(z, t)}{\partial z} = C_0 \frac{\partial U(z, t)}{\partial t} - G_0 U(z, t), \tag{5}$$

Thus, the current changes along a homogeneous section, since one part of the current in the form of a leakage current passes to the external conductor and the other part of the current increases the charge of the section and closes between the conductors in the form of a displacement current.

Thus, we can use these differential equations for a homogeneous section of the coaxial line in the quasi-static approximation, which we consider for a time-harmonic process.

2.3. Solution of Differential Equations for a Homogeneous Section of a Coaxial Line

Differentiating Equations (4) and (5), we derive two second-order partial differential equations, each containing only one variable. Voltage and current in the general case depend on both the spatial coordinate and on time; the functions expressing them according to the boundary conditions can be very complex.

In practice, the most important solutions are for sinusoidal functions of time, which can be represented as:

$$\tilde{U} = \dot{U}_0 e^{j\omega t - \gamma z}, \tag{6}$$

where γ is the propagation constant.

In this way, a general solution is obtained for the voltage wave and for the current wave:

$$\begin{aligned} \tilde{U}(z, t) &= \tilde{U}^+ + \tilde{U}^- = \dot{U}_0^+ e^{j\omega t - \gamma z} + \dot{U}_0^- e^{j\omega t + \gamma z}, \\ \tilde{I}(z, t) &= \tilde{I}^+ + \tilde{I}^- = \dot{I}_0^+ e^{j\omega t - \gamma z} + \dot{I}_0^- e^{j\omega t + \gamma z}. \end{aligned} \tag{7}$$

Thus, two voltage waves and two current waves propagate in the consideration system along the section of the coaxial line towards each other.

2.4. Derivation of an Expression for the Input Resistance of a Homogeneous Segment of a Coaxial Load for the Calculation of Equivalent Circuit Impedance

The load impedance is denoted by Z_L . Let l be the length of a homogeneous segment; Z_0 is its characteristic impedance, and Γ is the reflection coefficient:

$$\begin{aligned} Z_0 &= \sqrt{\frac{R_0 + j\omega L_0}{G_0 + j\omega C_0}}, \\ \Gamma &= \frac{Z_L - Z_0}{Z_L + Z_0}. \end{aligned} \tag{8}$$

Then the voltage at the transmission line point with coordinate z is:

$$\tilde{U} = \dot{U}_0^+ e^{j\omega t} (e^{-\gamma z} + \Gamma e^{\gamma z}), \tag{9}$$

and the current is:

$$\tilde{I} = \dot{I}_0^+ e^{j\omega t} (e^{-\gamma z} - \Gamma e^{\gamma z}). \tag{10}$$

Let us transform the formula for voltage:

$$\begin{aligned} \tilde{U} &= \dot{U}_0^+ e^{j\omega t} \left(\frac{e^{-\gamma z}}{2} + \frac{e^{-\gamma z}}{2} + \frac{\Gamma e^{\gamma z}}{2} + \frac{\Gamma e^{\gamma z}}{2} + \frac{e^{\gamma z}}{2} - \frac{e^{\gamma z}}{2} + \frac{\Gamma e^{-\gamma z}}{2} - \frac{\Gamma e^{-\gamma z}}{2} \right), \\ \tilde{U} &= \dot{U}_0^+ e^{j\omega t} \left[(\Gamma + 1) \frac{e^{\gamma z} + e^{-\gamma z}}{2} + (\Gamma - 1) \frac{e^{\gamma z} - e^{-\gamma z}}{2} \right], \text{ and finally} \\ \tilde{U} &= \dot{U}_0^+ (1 + \Gamma) e^{j\omega t} \left[ch(\gamma z) - \frac{1 - \Gamma}{1 + \Gamma} sh(\gamma z) \right] \end{aligned} \tag{11}$$

If we place the load at the point $z = 0$, then the voltage and amplitude of the incident wave are related by the equality:

$$\dot{U}_L = \dot{U}_0^+ (1 + \Gamma), \tag{12}$$

Then, we find that:

$$\tilde{U} = \dot{U}_L e^{j\omega t} \left[ch(\gamma z) - \frac{1 - \Gamma}{1 + \Gamma} sh(\gamma z) \right]. \tag{13}$$

The current at the point $z = 0$ can be expressed as:

$$\dot{I}_L = \dot{I}_0^+ + \dot{I}_0^- = \dot{U}_0^+ \left(\frac{1 - \Gamma}{Z_0} \right) = \frac{\dot{U}_L}{1 + \Gamma} (1 - \Gamma) \frac{1}{Z_0} = \frac{\dot{U}_L}{Z_0} \frac{1 - \Gamma}{1 + \Gamma} \tag{14}$$

From (13), we obtain the voltage vector at an arbitrary point:

$$\dot{U} = \dot{U}_L ch(\gamma z) - \dot{I}_L Z_0 sh(\gamma z). \tag{15}$$

Similarly, for the current, we find:

$$\dot{I} = \dot{I}_L ch(\gamma z) - \frac{\dot{U}}{Z_0} sh(\gamma z). \tag{16}$$

If we move to the z' coordinate, counted not from the end, but from the input of a homogeneous segment, that is, $z' = l + z$ at $0 > z > -l$, then, for voltage and current, we obtain the expressions:

$$\begin{aligned} \dot{U} &= \dot{U}_L ch(\gamma(l - z')) + \dot{I}_L Z_0 sh(\gamma(l - z')), \\ \dot{I} &= \dot{I}_L ch(\gamma(l - z')) + \frac{\dot{U}}{Z_0} sh(\gamma(l - z')). \end{aligned} \tag{17}$$

Accordingly, the voltage and current at the input of a homogeneous segment, that is, at the point $z' = 0, z = -l$, are equal to:

$$\begin{aligned} \dot{U}_{in} &= \dot{U}_L ch(\gamma l) + \dot{I}_n Z_0 sh(\gamma l), \\ \dot{I}_{in} &= \dot{I}_L ch(\gamma l) + \frac{\dot{U}}{Z_0} sh(\gamma l). \end{aligned} \tag{18}$$

From Equation (31), we find the input impedance of a homogeneous segment with the assumption that a load impedance Z_{in} is connected to its end.

$$Z_{in} = \frac{\dot{U}_{in}}{\dot{I}_{in}} = \frac{\dot{U}_L ch(\gamma l) + \dot{I}_n Z_0 sh(\gamma l)}{\dot{I}_L ch(\gamma l) + \frac{\dot{U}_n}{Z_0} sh(\gamma l)} = \frac{Z_L ch(\gamma l) + Z_0 sh(\gamma l)}{ch(\gamma l) + \frac{Z_L}{Z_0} sh(\gamma l)}. \tag{19}$$

If we neglect the losses in the coaxial load, then the input impedance of a homogeneous segment can be written as:

$$Z_{in} = Z_0 \frac{Z_L \cos(\beta l) + j Z_0 \sin(\beta l)}{Z_0 \cos(\beta l) + j Z_L \sin(\beta l)}. \tag{20}$$

After dividing the numerator and denominator on the right side of expression (20) by $\cos(\beta l)$, for the input impedance, we obtain the following expression:

$$Z_{in} = Z_0 \frac{Z_L + j Z_0 \operatorname{tg}(\beta l)}{Z_0 + j Z_L \operatorname{tg}(\beta l)}. \tag{21}$$

Expression (21) is the basis for the analysis of the equivalent circuit of the coaxial load on the microwave. However, this method can be used in the frequency range in which the conditions of quasi-stationarity (1) and (2) are satisfied.

2.5. Solution of an Electrodynamics Problem for a Homogeneous Segment of a Coaxial Load, Considering Heat Losses

The analysis was carried out by the successive approximation method. In the first approximation, heat losses are not taken into account. In this case, we assume that the depth of the skin layer $\delta = 0$, that is, we consider the currents as surface, which facilitates the solution of the problem. In the second approximation, for the field outside the conductors, the values obtained in the first approximation are accepted. These values serve as boundary conditions for determining the field inside the conductors, by determining which, the heat losses and, at the same time, the attenuation of the waves along a homogeneous coaxial load segment with equivalent parameters, can be found.

The problem is solved by introducing a cylindrical coordinate system r, α, z , in which the z axis is directed along the coaxial load axis.

A homogeneous section of a coaxial load with equivalent dimensions and medium parameters is assumed to have axial symmetry, so the field in it will also be axially symmetric; that is, the field strength and the density of surface currents will not depend on the polar angle.

Solving this problem, we obtain expressions for the field components [27]:

$E_r = \frac{A_0}{r} e^{j(\omega t - kz)} + \frac{A'_0}{r} e^{j(\omega t + kz)}$. The first term of this expression is a wave propagating in the positive direction of the z -axis, and the second is a wave propagating in the opposite direction. These waves are independent of each other, so that we can confine ourselves to considering only one of them, for example, the first one, and put $A'_0 = 0$ and:

$$E_r = \frac{A_0}{r} e^{j(\omega t - kz)}. \tag{22}$$

Second, we can obtain:

$$H_\alpha = \sqrt{\frac{\epsilon}{\mu}} E_r = \sqrt{\frac{\epsilon}{\mu}} \frac{A_0}{r} e^{j(\omega t - kz)}. \tag{23}$$

Next, by using the boundary conditions, we obtain:

$$\begin{cases} \tau_1 = \frac{\varepsilon A_0}{d} e^{j(\omega t - kz)}; \tau_2 = \frac{\varepsilon A_0}{D} e^{j(\omega t - kz)} \\ j_1 = \sqrt{\frac{\varepsilon}{\mu}} \frac{A_0}{d} e^{j(\omega t - kz)}; j_2 = \sqrt{\frac{\varepsilon}{\mu}} \frac{A_0}{D} e^{j(\omega t - kz)} \end{cases} \quad (24)$$

The strength of the currents flowing through the central and outer conductors is equal to the product of the surface current density and the circumference of the central and outer conductors, respectively:

$$\begin{cases} I_1 = j_1 \pi d = \pi \sqrt{\frac{\varepsilon}{\mu}} A_0 \cos(\omega t - kz); \\ I_2 = j_2 \pi D = -\pi \sqrt{\frac{\varepsilon}{\mu}} A_0 \cos(\omega t - kz) \end{cases} \quad (25)$$

Here (and henceforth), the index 1 corresponds to the central conductor and index 2 corresponds to the outer conductor.

Let us move on to the second approximation, which considers the penetration of the field into the conductors. Of practical interest are not the exact values of the field in the conductors, but, instead, the energy loss and damping of the wave as it propagates along the coaxial load. If the thickness of the conductive layer (skin layer) is:

$$\delta = \frac{1}{p} = \sqrt{\frac{2}{\omega \mu_0 \mu_r \sigma}} \quad (26)$$

much smaller than the dimensions d and D , then the surface curvature of the equivalent load segment will not affect the distribution of currents in the conductive layer. Therefore, the formula for the case of a flat surface of the conductor can be used, for which: $i = i_0 e^{-p\xi} \cos(\omega t - p\xi)$, where i_0 is the amplitude of the bulk current density on the conductor surface $\xi = 0$, and ξ is the coordinate directed normally inward conductor. If we replace this volume distribution of currents with the surface distribution of currents, then the density of the equivalent surface current j is equal to:

$$j = \int_0^\infty i d\xi = i_0 \int_0^\infty e^{-p\xi} \cos(\omega t - p\xi) d\xi = \frac{i_0}{p\sqrt{2}} \cos(\omega t - \frac{\pi}{4}) \quad (27)$$

Thus, the amplitude of the equivalent surface current is: $j_0 = \frac{i_0}{p\sqrt{2}}$.

Next, we calculate the amount of heat released per unit time per unit area in the surface layer of the conductor and average the value obtained over the field period:

$$q = \frac{1}{\sigma} \left(\int_0^\infty i d\xi \right)^2 = \frac{i_0^2}{\sigma} \left(\int_0^\infty e^{-p\xi} \overline{\cos(\omega t - p\xi)} d\xi \right)^2 = \frac{i_0^2}{4p^2\sigma} \quad (28)$$

Or, expressing i_0 in terms of j_0 :

$$q = \frac{j_0^2}{2\sigma} \quad (29)$$

This formula expresses heat losses in microwave fields in terms of the surface current density amplitude, to determine which, it is sufficient to solve the problem of propagation along the conductors in the first approximation, assuming the conductors are ideal.

The amplitude of the surface current density on the equivalent central conductor surface is $j_{01} = \sqrt{\frac{\varepsilon}{\mu}} \frac{A_0}{d}$.

Therefore, per unit of time and per unit length of the central conductor, the equivalent surface of which is πd , heat is released $Q_1 = \frac{\pi \varepsilon \rho_1 A_0^2}{\mu \sigma_1 d}$, where the index "1" of the values σ

and p means that they are related to the center conductor. A similar expression is obtained for the heat Q_2 released in the outer conductor, so that the total heat loss per unit length is:

$$Q = Q_1 + Q_2 = \frac{\pi \epsilon A_0^2}{\mu} \left(\frac{p_1}{\sigma_1 d} + \frac{p_2}{\sigma_2 D} \right). \tag{30}$$

Let us calculate the energy flux Σ , averaged over the period, carried by the wave per unit time through the section of a homogeneous equivalent segment: $\Sigma = \int_d^D S_z 2\pi r dr = 2\pi \int_d^D \overline{E_r H_\alpha} r dr$, where S_z is the component of the Poynting vector $\vec{S} = [\vec{E}, \vec{H}]$, and where it is taken into account that, in the first approximation, according to (38), $H_r = H_\alpha = 0$. When determining the product $E_r H_\alpha$, we pass to the real parts of complex expressions (41), (42), and then obtain: $\overline{E_r H_\alpha} = \sqrt{\frac{\epsilon}{\mu}} \frac{A_0^2}{r^2} \cos^2(\omega t - kz) = \sqrt{\frac{\epsilon}{\mu}} \frac{A_0^2}{2r^2}$, therefore:

$$\Sigma = \pi \sqrt{\frac{\epsilon}{\mu}} A_0^2 \int_d^D \frac{dr}{r} = \pi \sqrt{\frac{\epsilon}{\mu}} A_0^2 \ln\left(\frac{D}{d}\right). \tag{31}$$

The thermal losses Q must cause the wave to attenuate; that is, they must lead to the dependence of its amplitude on the z coordinate. This dependence can be determined from the fact that the heat $Q dz$ released per unit time on a segment of length dz must be equal to the difference in energy flows through two sections that limit this segment:

$$\Sigma - (\Sigma + d\Sigma) = Q dz, \text{ or } \frac{d\Sigma}{dz} = -Q. \tag{32}$$

Entering the values of Q and Σ into (31) from expressions (29), (30), and substituting the values of the constants p_1 and p_2 from expression (45), we obtain:

$$\begin{aligned} \frac{d}{dz} \left(\pi \sqrt{\frac{\epsilon}{\mu}} A_0^2 \ln\left(\frac{D}{d}\right) \right) &= -\frac{\pi \epsilon A_0^2}{\mu} \left(\frac{p_1}{\sigma_1 d} + \frac{p_2}{\sigma_2 D} \right), \\ \pi \sqrt{\frac{\epsilon}{\mu}} \ln\left(\frac{D}{d}\right) \frac{dA_0^2}{dz} &= -\frac{\pi \epsilon}{\mu} \left(\sqrt{\frac{\omega \mu_1 \sigma_1}{2}} + \sqrt{\frac{\omega \mu_2 \sigma_2}{2}} \right) A_0^2, \\ \frac{dA_0^2}{dz} &= -s A_0^2. \end{aligned} \tag{33}$$

From the last Equation (33), one can obtain an expression for the wave attenuation coefficient s :

$$s = \frac{\sqrt{\frac{\epsilon \omega}{2\mu}}}{\ln\left(\frac{D}{d}\right)} \left(\sqrt{\frac{\mu_1}{\sigma_1}} + \sqrt{\frac{\mu_2}{\sigma_2}} \right). \tag{34}$$

Thus, when thermal losses are taken into account, the amplitude of the wave propagating along a homogeneous equivalent segment of the coaxial load decays according to the law:

$$A_0 = a_0 e^{-sz}, \tag{35}$$

where a_0 is a coefficient defined for each coaxial line design.

Figure 1 shows the frequency dependence of the wave attenuation coefficient, calculated by formula (34), for various diameters of the outer and inner conductors of the coaxial line.

As can be seen from the graphs, the attenuation coefficient of the wave increases with increasing frequency. The ratio of the diameters of the outer and inner conductors of the coaxial line has little effect on the change in the attenuation coefficient of the wave.

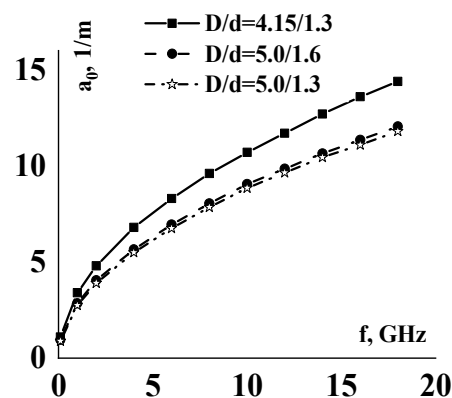


Figure 1. Frequency dependence of the wave attenuation coefficient for various diameters of the outer and inner conductors of the coaxial line.

3. Mathematical Model of a Coaxial Matched Load, Considering the Influence of Its Design and Technological Parameters in the Microwave Range

3.1. Accounting for Inhomogeneities of the Coaxial Load at Microwave

Load designs and their production technology lead to inhomogeneities that affect the propagation of electromagnetic waves [28]. If an inhomogeneity is introduced into the transmission line, then the primary field near it is distorted. The new field decomposes into an incident wave, two scattered waves propagating in opposite directions, and a series of rapidly damped oscillations of higher types [29]. The inhomogeneity behaves like reactive conduction due to the energy reserve in these higher modes of oscillation. Inhomogeneity is equivalent to capacitance or inductance, depending on whether the energy stored by the electric field exceeds the energy stored by the magnetic field. At microwave wavelengths the effect of inhomogeneities have a shunting effect and contribute to the emergence of parasitic oscillations of higher types of waves.

Analysis of inhomogeneities [30] and their quantitative assessment are possible if the energy transmission line type is specified. In this paper, these problems are solved in relation to a coaxial transmission line with a small-sized resistor as a termination.

The effect of inhomogeneities can be considered using an equivalent scheme of lumped constants [29]. This can be applied at any fixed frequency, but, in general, as the frequency changes, the parameters of the equivalent circuit will change. As a rule, the effect of inhomogeneities is considered at the central frequency of the operating range. The equivalent circuit also depends on which planes are chosen as reference planes.

If the longitudinal dimensions of the inhomogeneity are small compared to the wavelength, then an equivalent circuit can be used in the form of a parallel-connected reactivity connected directly at the location of the inhomogeneity. In the case when the thickness of the inhomogeneity is finite and the reference plane is chosen at the center of the inhomogeneity, the equivalent circuit will be a more complex T- or U-shaped circuit, which, as the thickness of the inhomogeneity tends to zero, approaches a simple parallel reactivity. The equivalent circuit also changes when two inhomogeneities are so close to each other that interaction between the emerging higher modes of vibration becomes possible.

Coaxial matched load consists of a transmission line segment with an absorbing element. A small lumped resistor acts as an absorbing element. For matching in a wide frequency band, a resistor is installed at the end of a regular short-circuited coaxial transmission line.

Inhomogeneities arise in places where the impedance changes. Figure 2 shows the design of the coaxial matched load as one option. However, with this design, it is not possible to fix the center conductor of the coaxial line. Therefore, at the place where the resistor was installed, it was necessary to abruptly increase the dimensions of the coaxial line (section T₂), which led to the appearance of inhomogeneity.

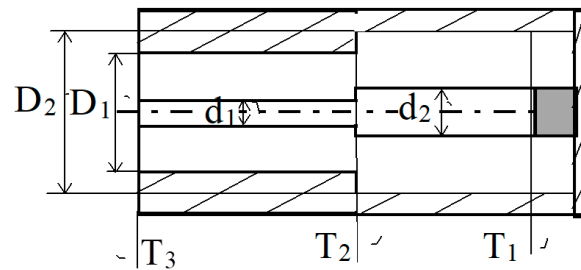


Figure 2. The scheme of coaxial load.

The jump in the coaxial line size in the section T_2 is due to design features and has a capacitive character.

Figure 3 shows the equivalent circuit of this load.

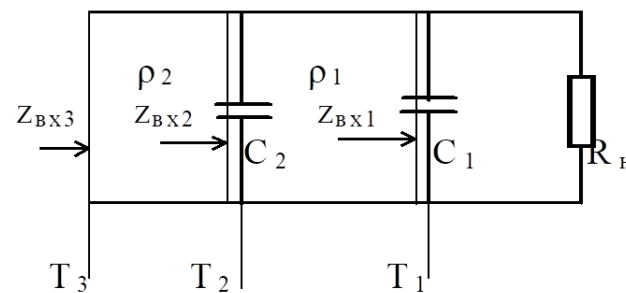


Figure 3. Equivalent circuit of coaxial load.

The value of the shunt capacitance C_2 can be determined by the method proposed in [28]:

$$C_2 = C_a + C_b, \text{ where}$$

$$C_a = 2\pi D_1 S_1(\alpha; \beta);$$

$$C_b = 2\pi D_2 S_2(\alpha; \beta);$$

$$\alpha = (D_2 - D_1) / (d_2 - d_1);$$

$$\beta = \frac{D_1}{d_1}.$$

Parameters $S_1(\alpha; \beta)$; $S_2(\alpha; \beta)$ are determined in [29].

The capacitance value C_1 is calculated by the formula for the capacitance of a flat capacitor: $C_1 = (0.885\epsilon \cdot l \cdot b) / h$, where l, b, h are expressed in millimeters.

Thus, having calculated the capacitances value, we considered the inhomogeneities of the coaxial load.

3.2. Calculation of Voltage Standing Wave Ratio and Attenuation of Microwave Oscillations in a Coaxial Transmission Line with a Resistor as a Termination

To optimize the design of the developed microwave loads [31], it is necessary to know the analytical expression for the attenuation and the voltage standing wave ratio (VSWR) in the transmission line with a built-in resistor.

The attenuation can be calculated if the analytical expression for the impedance is known. When calculating the impedance, the following assumptions were made:

- a T-type wave propagates along a coaxial line in the microwave range;
- the thermal and dielectric losses due to their smallness are neglected;
- inhomogeneities are capacitive in nature.

These assumptions make it possible to represent the equivalent load circuit in the form of an inhomogeneous transmission line, composed of homogeneous sections with a change in impedance at the interface, considering shunt capacitances (see Figure 3).

The wave resistances of the homogeneous sections coaxial line are expressed in terms of design parameters by the following relations [27,32]: $\rho_1 = \frac{60}{\sqrt{\epsilon}} \ln \frac{D_2}{d_2}$; $\rho_2 = \frac{60}{\sqrt{\epsilon}} \ln \frac{D_1}{d_1}$, and $R_L = 50 \text{ Ohm}$; here, ϵ is the relative permittivity of the coaxial line filling.

To calculate the input impedance of the device, the method of impedance transformation by segments of homogeneous sections of the transmission line is used. The input impedance in the section T₁ is [33]:

$$Z_{in1} = \frac{R_L}{(1 + j\omega C_1 \frac{R_L}{3})}, \text{ or } Z_{in1} = a_1 - jb_1. \tag{36}$$

The input impedance in the section T₂ is:

$$Z_{in2} = a_2 - jb_2, \tag{37}$$

where:

$$\begin{aligned} a_2 &= \frac{a_1\rho_1^2 + a_1\rho_1^2 \text{tg}^2[\beta(l_2 - l_1)]}{N_2 + M_2}, \\ b_2 &= \frac{D_2 + E_2 + F_2}{N_2 + M_2}, \\ D_2 &= \omega C_2 a_1^2 \rho_1^2 + a_1^2 \rho_1 \text{tg}[\beta(l_2 - l_1)] + \omega C_2 b_1^2 \rho_1 - \omega C_2 b_1 \rho_1^3 \text{tg}[\beta(l_2 - l_1)], \\ E_2 &= b_1 \rho_1^2 + b_1^2 \rho_1 \text{tg}[\beta(l_2 - l_1)] - \omega C_2 b_1 \rho_1^3 \text{tg}[\beta(l_2 - l_1)], \\ F_2 &= \omega C_2 \rho_1^4 \text{tg}^2[\beta(l_2 - l_1)] - \rho_1^3 \text{tg}[\beta(l_2 - l_1)] - b_1 \rho_1^2 \text{tg}^2[\beta(l_2 - l_1)], \\ N_2 &= \{ \omega C_2 b_1 \rho_1 - \omega C_2 \rho_1^2 \text{tg}[\beta(l_2 - l_1)] + \rho_1 + b_1 \text{tg}[\beta(l_2 - l_1)] \}^2, \\ M_2 &= \{ \omega C_2 a_1 \rho_1 + a_1 \text{tg}[\beta(l_2 - l_1)] \}^2. \end{aligned}$$

The input impedance in the section T₃ is:

$$Z_{in3} = a_3 - jb_3, \tag{38}$$

where: $a_3 = \frac{a_2\rho_2^2 + a_2\rho_2^2 \text{tg}^2[\beta(l_3 - l_2)]}{\{ \rho_2 + b_2 \text{tg}[\beta(l_3 - l_2)] \}^2 + a_2^2 \text{tg}^2[\beta(l_3 - l_2)]},$

$$\begin{aligned} b_3 &= \frac{a_2^2 \rho_2 \text{tg}[\beta(l_3 - l_2)] + b_2^2 \rho_2 \text{tg}[\beta(l_3 - l_2)] - D_3}{\{ \rho_2 + b_2 \text{tg}[\beta(l_3 - l_2)] \}^2 + a_2^2 \text{tg}^2[\beta(l_3 - l_2)]}, \\ D_3 &= \rho_2^3 \text{tg}[\beta(l_3 - l_2)] + b_2 \rho_2^2 \text{tg}^2[\beta(l_3 - l_2)]. \end{aligned}$$

Reflection coefficient in section T₃:

$$\dot{\Gamma} = Q - jP, \tag{39}$$

where $Q = \frac{a_3^2 + b_3^2 - R_L^2}{(a_3 + R_L) + b_3^2}, P = \frac{2R_L b_3}{(a_3 + R_L) + b_3},$ and the reflection coefficient modulus is

$$|\dot{\Gamma}| = \sqrt{Q^2 + P^2}.$$

The VSWR is given by expression:

$$\text{VSWR} = \frac{1 + |\dot{\Gamma}|}{1 - |\dot{\Gamma}|} \tag{40}$$

Attenuation is given by expression:

$$A = 10 \cdot \lg \frac{(\text{VSWR} + 1)^2}{4 \cdot \text{VSWR}}, \tag{41}$$

Here, in all expressions ω —circular frequency; β —phase factor without considering energy losses in the dielectric; λ —wavelength in the line; and C_1 and C_2 are shunt capacitances.

3.3. Influence Compensation of Shunt Capacitances in Order to Improve Coaxial Load Matching over a Wide Frequency Range

Shunt capacitance compensation can be performed by introducing a series inductance into the coaxial transmission line. The inductance can be made structurally in the form of a coaxial line segment with a high impedance of length $l_L \ll \Lambda/4$, where Λ is the wavelength in the transmission line. Such inductance is obtained by shifting the jumps of the outer and inner conductors of the coaxial line. Figure 4 shows the design of the matched load.

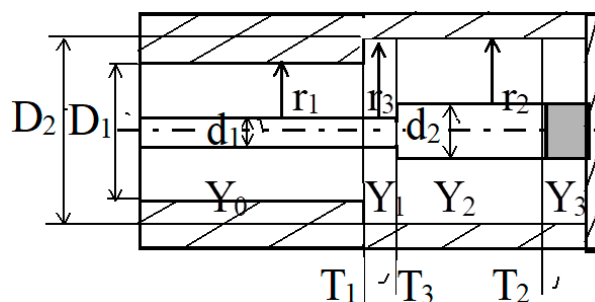


Figure 4. Design of a coaxial matched load with a compensating element.

Figure 5 shows the equivalent load circuit with compensating inductance L_k .

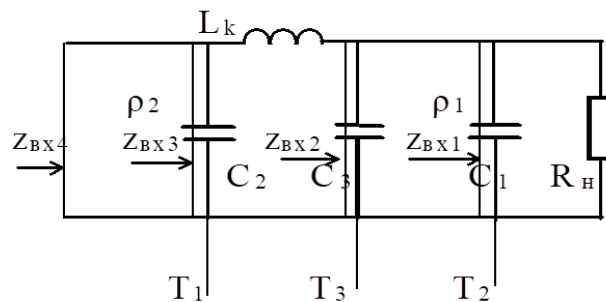


Figure 5. Equivalent load circuit with compensating inductance L_k .

The value of the compensating inductance is determined from the condition of ensuring resonance at the upper frequency of the load operating range: $L_k = 1/(\omega^2 C^*)$, where C^* is the total capacitance. Linear inductance is determined by the formula [29]: $L_{II} = (\mu_0/2\pi) \ln(D_2/d_1)$, where: $\mu_0 = 4\pi \cdot 10^{-7}$ H/m.

4. Experimental Research of the Coaxial Load Matching Degree in the Range of 0.1 ... 18 GHz

4.1. Description of Load Design

To experimentally verify the results obtained, as well as to evaluate the influence of the manufacturing accuracy of structural elements on the electrical characteristics, a broadband coaxial load based on a small-sized resistor was developed [34,35].

In general, the load should contain a high-frequency connector (socket or plug) [36] for connection with the device and a segment of the transmission line with an absorbing element. From the point of view of minimizing the load size, it is advisable to use a small-sized lumped resistor as an absorbing element.

To ensure matching in a wide frequency band, a resistor must be installed at the end of a short-circuited coaxial line. In view of the foregoing, the design of the load has the form shown in Figure 6.

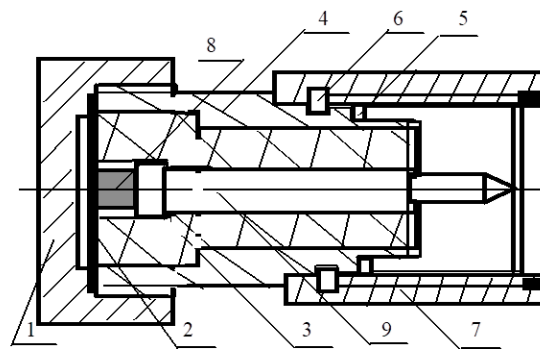


Figure 6. Scheme of coaxial matched load. 1. Lid. 2. Washer. 3. Insulator (PTFE F-4, $\varepsilon = 2$). 4. Body. 5. Rubber ring. 6. Metal ring. 7. Nut. 8. Resistor C-6-9 (50 Ohm; 125 mW). 9. Rod.

A standard small-sized coaxial 50-ohm connector [31] with a cross-section of 4.15×1.3 mm with PTFE filling was used to connect to external devices. A coaxial line with the same cross-section serves as a continuation of the connector, which makes it possible to ensure high-quality matching at the interface due to the regularity of the electromagnetic field structure. To ensure fixation of the central conductor of the coaxial line, its dimensions at the place where the resistor is installed are abruptly increased to a cross-section of 5.0×1.6 mm.

A miniature resistor C6-9-50 Ohm-0.125 W was chosen as an absorbing element. The resistor is made using thin-film technology on a polycor substrate $1 \times 1 \times 1$ mm in size with $\varepsilon = 9.8 \pm 0.2$. The resistive layer is deposited on one of the faces, the metallized contact pads are located on the opposite faces and tinned for soldering, which is convenient for installing the resistor in the coaxial transmission line.

The parasitic capacitance of the resistor C_1 , calculated by the formula for the capacitance of a flat capacitor, was 0.085 pF. The values of the shunt capacitances C_2 and C_3 , according to the numerical calculations, were 0.075 pF and 0.09 pF, respectively. Thus, the total capacitance C^* is 0.25 pF. The value of the compensating inductance, determined from the condition of ensuring resonance at the upper frequency of the operating range, is 0.31 nH. With the given dimensions of the device, the length of the compensating inductive element is 1.1 mm.

4.2. Data of Experimental Research of Coaxial Load

One of the most important requirements for microwave coaxial loads [37] is the degree of matching when they are connected to the transmission line. Matching provides full or partial compensation of the wave reflected by the load in the transmission line.

The matched mode is the mode in which the load impedance is equal to the characteristic impedance of the transmission line. VSWR is the parameter by which it is unambiguously possible to determine the degree of load matching with the transmission line. The modulus of the reflection coefficient is expressed in terms of VSWR by the formula:

$$|\Gamma| = \frac{\text{VSWR} - 1}{\text{VSWR} + 1}, \quad (42)$$

The experimental study and measurement of load characteristics was carried out on a vector network analyzer.

An experimental batch of developed coaxial loads was studied in the frequency range of 0.1–18.0 GHz. According to reference data [29], the use of small-sized resistors with a resistive film length not exceeding one millimeter as a terminator makes it possible to obtain a VSWR of 1.1–1.4 up to frequencies of 12–18 GHz.

Experimental research shows that, across almost the entire frequency range, the VSWR of the load lies in the range of 1.06–1.12 (Figure 7), which corresponds to 3–6% of the incident power reflection.

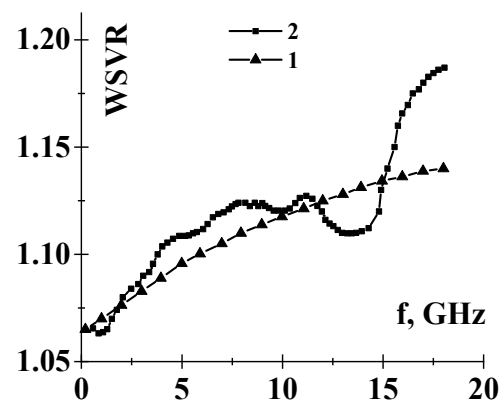


Figure 7. Frequency dependence of VSWR. 1-theoretical curve, 2-experimental curve.

The VSWR increase in the region of 16–18 GHz is because, at these frequencies, the dimensions of the resistor and the device, as a whole, become commensurate with the wavelength in the line. So, the total length of the device is about 12 mm, and the wavelength in the coaxial line filled with fluoroplast at a frequency of 18 GHz is equal to 11.8 mm and the resistor length is equal to 5.3 mm.

Therefore, at microwave wavelengths, distributed parameters begin to play a role, which were not considered before. However, even with a VSWR equal to 1.2, only 9% of the incident energy is reflected.

Losses in a coaxial line, as can be seen from the graph shown in Figure 8, also increase with increasing frequency.

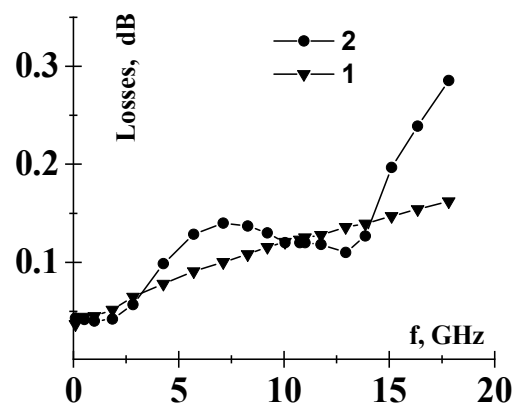


Figure 8. Frequency dependence of losses. 1-theoretical curve, 2-experimental curve.

Moreover, the nature of growth is the same as that of the VSWR. In the region of 16–18 GHz, there is a jump in losses on the experimental curve, which, as in the case of VSWR, is associated with distributed parameters. The numerical value of losses is small and ranges from 0.05 dB in the low-frequency region to 0.3 dB for the upper frequencies of the range. The measurements were carried out on an Agilent vector network analyzer N5230A (108 dB of dynamic range and <0.006 dB trace noise) with calibration performed in the measurement plane. This ensured the low indicated losses.

5. Conclusions

The paper presents a theoretical method for research into coaxial microwave devices, on the basis of which a mathematical model is obtained. The calculation of heat losses for a homogeneous segment of the coaxial line is given. Analytical dependences of parasitic reactivity are obtained considering higher types of waves and the design and technological parameters of coaxial devices.

The theoretical discussion and experimental research presented in this paper allow us to conclude that it is possible to apply the classical theory of circuits in the calculation and design of coaxial broadband microwave devices under quasi-stationarity conditions.

The problem was solved by considering Maxwell's equations in a region bounded by a conducting surface with boundary conditions specified on it, relating electric and magnetic fields to the surface densities of electric currents and charges or to the surface impedance. Differential equations are obtained and solved for a homogeneous section of a coaxial line in the quasi-static approximation.

The resulting mathematical model allows us to represent a coaxial device in the form of a cascade connection of transmission line homogeneous segments, considering reactive inhomogeneities in places where the impedance changes. The influence of shunting inhomogeneities can be compensated for by introducing additional elements.

Small-sized lumped elements with insignificant reactivity, which can be compensated for in a wide frequency band, make it possible to obtain devices with a VSWR not exceeding 1.2.

The proposed method can be applied to the design and development of various types of coaxial devices at microwave wavelengths.

Author Contributions: Conceptualization and review and editing of the paper was undertaken by A.S.T.; Section 2: "Theoretical method of research coaxial load at microwave" was written by P.V.T.; Section 3: "Mathematical model of a coaxial matched load" was written jointly by A.S.T. and P.V.T.; Section 4: "Experimental research of the coaxial load" and the conclusion were written by A.S.T. All authors have read and agreed to the published version of the manuscript.

Funding: This research received no external funding.

Data Availability Statement: Not applicable.

Conflicts of Interest: The authors declare no conflict of interest.

References

1. Smyth, B.P.; Iyer, A.K. Embedded MTM-EBGs in patch antenna for simultaneously dual-band and dual-polarized operation. In Proceedings of the 2020 14th European Conference on Antennas and Propagation (EuCAP), Copenhagen, Denmark, 15–20 March 2020; pp. 1–4. [\[CrossRef\]](#)
2. Ibrahim, M.Y.; Ashyap, A.Y.I.; Abidin, Z.Z.; Dahlan, S.H. Implementation of electromagnetic band-gap structure in antenna applications: An overview. In Proceedings of the 2020 IEEE Student Conference on Research and Development (SCORED), Batu Pahat, Malaysia, 27–29 September 2020; pp. 33–38. [\[CrossRef\]](#)
3. Kiani, S.H.; Altaf, A.; Abdullah, M.; Muhammad, F.; Shoaib, N.; Anjum, M.R.; Damaševicius, R.; Blažauskas, T. Eight element side edged framed MIMO antenna array for future 5G smart phones. *Micromachines* **2020**, *11*, 956. [\[CrossRef\]](#)
4. Ahmad, K.S.; Aziz, M.Z.A.A.; Abdullah, N.B. Microstrip antenna array with defected ground structure and copper tracks for bandwidth enhancement. In Proceedings of the 2020 IEEE International RF and Microwave Conference (RFM), Kuala Lumpur, Malaysia, 14–16 December 2020; pp. 1–5. [\[CrossRef\]](#)
5. Abohmra, A.; Abbas, H.; Al-Hasan, M.; Mabrouk, I.B.; Alomainy, A.; Imran, M.A.; Abbasi, Q.H. Terahertz antenna array based on a hybrid perovskite structure. *IEEE Open J. Antennas Propag.* **2020**, *1*, 464–471. [\[CrossRef\]](#)
6. Yildiz, Ö.F.; Thomsen, O.; Bochar, M.; Yang, C.; Schuster, C. Vertically integrated microwave-filters using functional via structures in LTCC. In Proceedings of the 2020 50th European Microwave Conference (EuMC), Utrecht, The Netherlands, 12–14 January 2021; pp. 966–969. [\[CrossRef\]](#)
7. Fu, W.; Li, Z.M.; Chng, J.W.; Qiu, X. A review of microwave filter designs based on CMRC. In Proceedings of the 2020 IEEE MTT-S International Wireless Symposium (IWS), Shanghai, China, 20–23 September 2020; pp. 1–3. [\[CrossRef\]](#)
8. Geyikoglu, M.D.; Koc Polat, H.; Cavusoglu, B. Novel Design for differential phaseshifter structure by using multi-section coupled lines. *Electron. Lett.* **2020**, *56*, 553–556. [\[CrossRef\]](#)
9. Shao, C.; Chu, H.; Zhu, X.H. Continuously tunable phase shifter based on defected ground structures. In Proceedings of the 2020 IEEE MTT-S International Microwave Workshop Series on Advanced Materials and Processes for RF and THz Applications (IMWS-AMP), Suzhou, China, 29–31 July 2020; pp. 1–3. [\[CrossRef\]](#)
10. Abbasi, Z.; Baghelani, M.; Daneshmand, M. High-resolution chipless tag RF sensor. *IEEE Trans. Microw. Theory Tech.* **2020**, *68*, 4855–4864. [\[CrossRef\]](#)
11. Atkishkin, S. Flexible 3D slabline and stripline microwave delay lines on polymer substrate. In Proceedings of the 2020 International Conference on Actual Problems of Electron Devices Engineering (APEDE), Saratov, Russia, 24–25 September 2020; pp. 129–133. [\[CrossRef\]](#)

12. Tao, T.; Yang, J.; Wei, W.; Wozniak, M.; Scherer, R.; Damaševičius, R. Design of a MEMS sensor array for dam subsidence monitoring based on dual-sensor cooperative measurements. *KSII Trans. Internet Inf. Syst.* **2021**, *15*, 3554–3570.
13. He, X.; Kong, L.; Zhang, Y. Modelling of tunable CPW structure dielectric phase shifters. In Proceedings of the 2020 IEEE 3rd International Conference on Electronic Information and Communication Technology (ICEICT), Shenzhen, China, 13–15 November 2020; pp. 368–371. [[CrossRef](#)]
14. Wang, Y.; Wang, X.; Wang, Y.; Yu, C.; Zhang, W.; Liang, F.; Zhang, Z.; Gao, S.; Chen, J. Reconfigurable microwave phase shifter based on nematic liquid crystal: Design and experimental validation. In Proceedings of the 2020 IEEE 3rd International Conference on Electronic Information and Communication Technology (ICEICT), Shenzhen, China, 13–15 November 2020; pp. 455–459. [[CrossRef](#)]
15. Liu, S.; Zhang, G.; Wan, T.; Hu, Y. Numerical simulation of electromagnetic-thermal effect of microwave devices. In Proceedings of the 2019 International Applied Computational Electromagnetics Society Symposium—China (ACES), Nanjing, China, 8–11 August 2019; Volume 1, pp. 1–2. [[CrossRef](#)]
16. Flynn, D.; Marpe, D.; Naccari, M.; Nguyen, T.; Rosewarne, C.; Sharman, K.; Sole, J.; Xu, J. Overview of the range extensions for the HEVC standard: Tools, profiles, and performance. *IEEE Trans. Circuits Syst. Video Technol.* **2016**, *26*, 4–19. [[CrossRef](#)]
17. Mejillones, S.C.; Oldoni, M.; Moscato, S.; Macchiarella, G. Analytical synthesis of fully canonical cascaded-doublet prototype filters. *IEEE Microw. Wirel. Compon. Lett.* **2020**, *30*, 1017–1020. [[CrossRef](#)]
18. Macchiarella, G.; Gentili, G.G.; Tomassoni, C.; Bastioli, S.; Snyder, R.V. Design of Waveguide filters with cascaded singlets through a synthesis-based approach. *IEEE Trans. Microw. Theory Tech.* **2020**, *68*, 2308–2319. [[CrossRef](#)]
19. Mokarram, A.; Abdipour, A.; Askarpour, A.N.; Mohammadzade, A.R. Time-domain signal and noise analysis of millimetre-wave/THz diodes by numerical solution of stochastic telegrapher’s equations. *IET Microw. Antennas Propag.* **2020**, *14*, 1012–1020. [[CrossRef](#)]
20. Marcuvitz, N. *Waveguide Handbook*, 1st ed.; McGraw Hill: New York, NY, USA, 1951.
21. Green, H.E. The numerical solution of some important transmission line problems. *IEEE Trans. Microw. Theory Tech.* **1965**, *13*, 676–692. [[CrossRef](#)]
22. Young, L. The practical realization of series-capacitive couplings for microwave filters. *Microw. J.* **1962**, *5*, 79.
23. Janssen, R. On the performance of the least squares method for waveguide junctions and discontinuities. *IEEE Trans. Microw. Theory Tech.* **1975**, *23*, 434–436. [[CrossRef](#)]
24. Whinnery, J.R.; Jarnieson, H.W.; Robbins, T.E. Coaxial line discontinuities. *Proc. IRE* **1944**, *32*, 695–709. [[CrossRef](#)]
25. Harvey, A.F. *Microwave Engineering*; Academic Press: New York, NY, USA, 1963.
26. Lebedev, I.A. Equations in full differentials of third order. *J. Min. Inst.* **2013**, *202*, 239.
27. Jackson, J.D. *Classical Electrodynamics*, 3rd ed.; Wiley-VCH: Weinheim, Germany, 1998; p. 832.
28. Bebikhov, Y.V.; Semenov, A.S.; Yakushev, I.A.; Kugusheva, N.N.; Pavlova, S.N.; Glazun, M.A. The application of mathematical simulation for solution of linear algebraic and ordinary differential equations in electrical engineering. *IOP Conf. Ser. Mater. Sci. Eng.* **2019**, *643*, 012067. [[CrossRef](#)]
29. Gunston, M.A.R. *Microwave Transmission Line Data*; Noble Publishing Corp.: Atlanta, GA, USA, 1997.
30. Trofimets, E.N.; Trofimets, V.Y. Computer modelling of physical processes described by parabolic type equations. *IOP Conf. Ser. Mater. Sci. Eng.* **2021**, *1047*, 012140. [[CrossRef](#)]
31. Skamyin, A.; Shklyarskiy, Y.; Dobush, V.; Dobush, I. Experimental determination of parameters of nonlinear electrical load. *Energies* **2021**, *14*, 7762. [[CrossRef](#)]
32. Nikol’skii, V.V.; Nikol’skaia, T.I. *Electrodynamics and Propagation of Radio Waves*, 3rd revised and enlarged ed.; Izdatel’stvo Nauka: Moscow, Russia, 1989; p. 544. (In Russian)
33. Mazepova, O.I.; Meshchanov, V.P.; Prokhorova, N.I.; Feldshtein, A.L.; Yavich, L.R. *Guide to the Elements of Strip Technology*; Feldstein, A.L.M., Ed.; Communication: Washington, DC, USA, 1978. (In Russian)
34. Kapralov, G.N.; Bichurin, M.I.; Fomin, O.G.; Tatarenko, A.S. Ultra-wideband matched load. *Bull. Novgorod State Univ.* **1999**, *13*, 10–13. (In Russian)
35. Bichurin, M.I.; Fomin, O.G.; Tatarenko, A.S.; Kapralov, G.N. Coaxial matched load. *Nauka Proizvodstvu* **2000**, *8*, 34–36. (In Russian)
36. Bryant, J.H. Coaxial transmission lines. Connectors, and components: A U.S. historical perspective. *IEEE Trans. MTT* **1984**, *32*, 970–982. [[CrossRef](#)]
37. Zvonarev, I.E.; Ivanov, S.L. Evaluation of losses in transmission of machinery for development of mineral deposits in conditions of variable load. *IOP Conf. Ser. Earth Environ. Sci.* **2017**, *87*, 022024. [[CrossRef](#)]